Article

Cell Reports

Ubiquitination of MBNL1 Is Required for Its Cytoplasmic Localization and Function in Promoting Neurite Outgrowth

Graphical Abstract

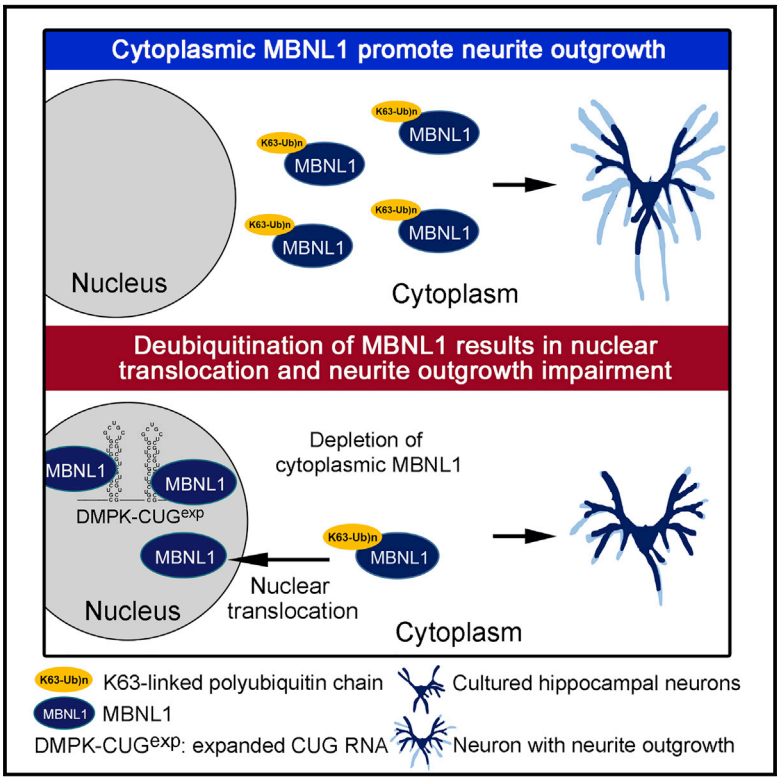

Authors

Pei-Ying Wang, Kuei-Ting Chang, Yu-Mei Lin, Ting-Yu Kuo, Guey-Shin Wang

Correspondence

gswang@ibms.sinica.edu.tw

In Brief

Wang et al. find that MBNL1 ubiquitination is required for cytoplasmic localization and promotion of neurite outgrowth. In myotonic dystrophy, expanded CUG repeat RNA leads to MBNL1 deubiquitination, resulting in nuclear-translocation-associated morphological defects that can be rescued by preventing degradation of lysine 63-linked polyubiquitin chains or enhancing MBNL1 ubiquitination.

Highlights

- Lysine 63-linked polyubiquitination regulates MBNL1 cytoplasmic localization
- Expanded CUG RNA leads to deubiquitination of cytoplasmic MBNL1
- MBNL1 deubiquitination results in nuclear translocation and morphological defects
- Inhibition of MBNL1 deubiquitination prevents morphological defects in DM1 neurons

Wang et al., 2018, Cell Reports *22*, 2294–2306
February 27, 2018
https://doi.org/10.1016/j.celrep.2018.02.025

CellPress

OPEN ACCESS
CellPress

Cell Reports
Article

Ubiquitination of MBNL1 Is Required for Its Cytoplasmic Localization and Function in Promoting Neurite Outgrowth

Pei-Ying Wang,[1,2] Kuei-Ting Chang,[2] Yu-Mei Lin,[2] Ting-Yu Kuo,[2] and Guey-Shin Wang[1,2,3,4,*]
[1]Program in Molecular Medicine, National Yang-Ming University and Academia Sinica, Taipei, Taiwan
[2]Institute of Biomedical Sciences, Academia Sinica, Taipei, Taiwan
[3]Taiwan International Graduate Program in Interdisciplinary Neuroscience, National Yang-Ming University and Academia Sinica, Taipei, Taiwan
[4]Lead Contact
*Correspondence: gswang@ibms.sinica.edu.tw
https://doi.org/10.1016/j.celrep.2018.02.025

SUMMARY

The Muscleblind-like protein family (MBNL) plays an important role in regulating the transition between differentiation and pluripotency and in the pathogenesis of myotonic dystrophy type 1 (DM1), a CTG expansion disorder. How different MBNL isoforms contribute to the differentiation and are affected in DM1 has not been investigated. Here, we show that the MBNL1 cytoplasmic, but not nuclear, isoform promotes neurite morphogenesis and reverses the morphological defects caused by expanded CUG RNA. Cytoplasmic MBNL1 is polyubiquitinated by lysine 63 (K63). Reduced cytoplasmic MBNL1 in the DM1 mouse brain is consistent with the reduced extent of K63 ubiquitination. Expanded CUG RNA induced the deubiqutination of cytoplasmic MBNL1, which resulted in nuclear translocation and morphological impairment that could be ameliorated by inhibiting K63-linked polyubiquitin chain degradation. Our results suggest that K63-linked ubiquitination of MBNL1 is required for its cytoplasmic localization and that deubiquitination of cytoplasmic MBNL1 is pathogenic in the DM1 brain.

INTRODUCTION

The Muscleblind-like protein family (MBNL), consisting of MBNL1, MBNL2, and MBNL3, encoded by three different genes, is evolutionarily conserved and multifunctional, involved in regulating alternative splicing, alternative polyadenylation, translation, mRNA localization, and miRNA processing (Charizanis et al., 2012; Rau et al., 2011; Wang et al., 2012). The MBNL protein family plays an important role in regulating the developmental alternative splicing transition that determines the choice between differentiation and pluripotency (Artero et al., 1998; Cheng et al., 2014; Han et al., 2013). MBNL proteins can promote the terminal differentiation of muscle cells and adipocytes as well as the differentiation and morphogenesis of *Drosophila* peripheral neurons (Pascual et al., 2006). Reduced expression of MBNL family proteins in differentiated cells enhances the pluripotency by reverting the targets to an embryonic-stem-cell-like alternative splicing pattern (Han et al., 2013; Holm et al., 2015).

Loss of MBNL function has been implicated in the neural pathogenesis of myotonic dystrophy (DM). The genetic basis of DM type 1 (DM1) involves an expansion of CTG repeats in the 3′ UTR of the Dystrophia Myotonia Protein Kinase (*DMPK*) gene. Accumulation of *DMPK* mRNA containing CUG repeats in the nuclear foci results in sequestration of MBNL protein because of similar affinities for CUG RNA repeats and its targets (Yuan et al., 2007), which leads to loss of nuclear function (Ho et al., 2004; Jiang et al., 2004; Suenaga et al., 2012). *Mbnl*-knockout mouse models, including $Mbnl1^{\Delta E3/\Delta E3}$ and $Mbnl2^{\Delta E2/\Delta E2}$, recapitulate several DM1 features, including misregulated alternative splicing and polyadenylation, defective motivation and spatial learning, and abnormal REM sleep propensity (Batra et al., 2014; Charizanis et al., 2012; Du et al., 2010; Goodwin et al., 2015; Kanadia et al., 2003), so MBNL dysfunction may contribute to the pathogenesis of the DM1 brain.

Characterization of MBNL family members by their affinity to target RNA and the association with expanded CUG RNA revealed that MBNL1 is required for RNA foci formation and exhibits the highest mobility to expanded CUG RNA (Querido et al., 2011; Sznajder et al., 2016). Hence, different MBNL members may exhibit distinct susceptibility to expanded CUG RNA, thereby contributing to different phenotypes. That MBNL1 has the highest binding and mobility to the target RNA and expanded CUG RNA suggests that MBNL1 is more susceptible to the pathogenic RNA than the other family members. In support of this notion, in a mouse model (EpA960/CaMKII-Cre) expressing expanded CUG RNA in the post-natal brain, reduced cytoplasmic MBNL1 expression on dendrites and dysfunction of synaptic transmission are the early events responding to the expression of expanded CUG RNA, whereas alteration of MBNL2-regulated alternative splicing is the later event (Wang et al., 2017), which also suggests that the causal mechanism leading to reduced cytoplasmic MBNL1 expression and MBNL2 dysfunction likely differs.

Different MBNL1 isoforms are generated from alternative splicing and localized in the cytoplasm and nucleus (Kanadia et al., 2006; Miller et al., 2000; Tran et al., 2011), but whether cytoplasmic and nuclear isoforms of MBNL1 have a similar function in

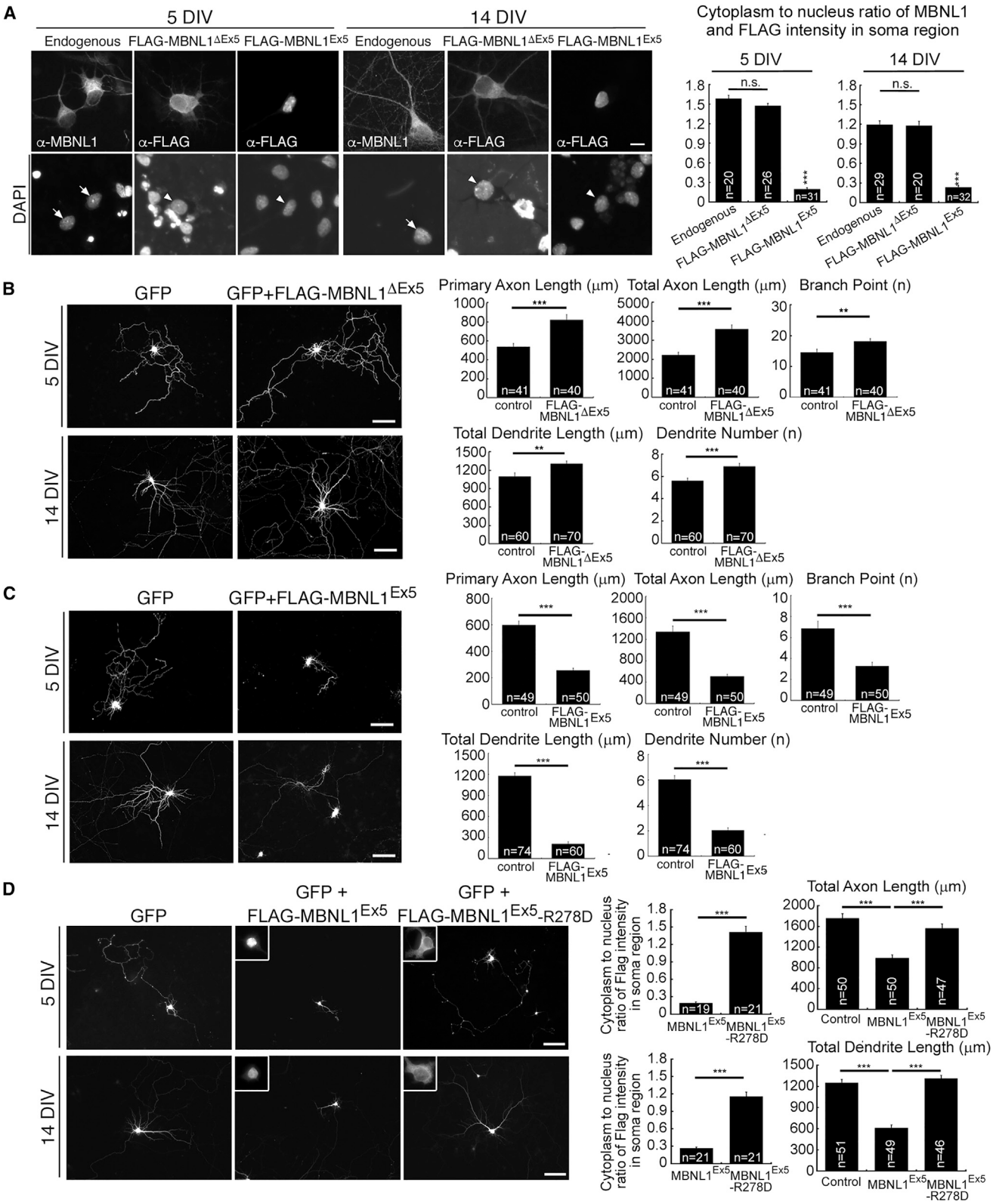

(legend on next page)

regulating differentiation has not been investigated. Sequestration of nuclear MBNL1 clearly results in loss of nuclear function, but how pathogenic RNA affects the cytoplasmic function of MBNL1 remains elusive. Cytoplasmic MBNL1 is not in close proximity to nuclear RNA foci, so the sequestration may be controlled by a different mechanism. Moreover, how the nucleocytoplasmic translocation of MBNL1 is regulated and whether reduced cytoplasmic MBNL1 expression in the EpA960/CaMKII-Cre brain is due to sequestration have not been investigated.

In the present study, we identified lysine 63 (K63)-linked ubiquitination as a regulatory mechanism for MBNL1 cytoplasmic localization in neurons. Pathogenic CUG RNA repeats induced deubiquitination of cytoplasmic MBNL1, thereby resulting in nuclear translocation and loss of its function in regulating neurite outgrowth, which could be ameliorated by inhibiting K63-linked polyubiquitin chain degradation or sustaining MBNL1 ubiquitination.

RESULTS

MBNL1 Cytoplasmic Isoform Enhances Neurite Outgrowth

To determine the effect of different MBNL1 isoforms on morphological differentiation, we used two constructs expressing spliced variants with or without exon 5 inclusion that were FLAG tagged: FLAG-MBNL1^{Ex5}, FLAG-MBNL1$^{\Delta Ex5}$. The *Mbnl1* exon 5-encoded segment Ex5 determines nuclear localization (Tran et al., 2011), so MBNL1$^{\Delta Ex5}$ and MBNL1^{Ex5} represent cytoplasmic and nuclear isoforms, respectively. We used cultured hippocampal neurons to examine the effect of MBNL1$^{\Delta Ex5}$ and MBNL1^{Ex5} expression on axon and dendrite morphology. The construct expressing MBNL1$^{\Delta Ex5}$ or MBNL1^{Ex5} was independently co-transfected with a GFP expression construct into hippocampal neurons at days 2 and 11 of *in vitro* culture (DIV). Axon outgrowth and dendrite development were analyzed at 5 and 14 DIV, respectively, with GFP expression used to show the morphology of neurons.

We first examined the effect of the FLAG-MBNL1$^{\Delta Ex5}$ expression on neurite outgrowth. Consistent with endogenous MBNL1, in cultured hippocampal neurons at 5 and 14 DIV, overexpressed FLAG-MBNL1$^{\Delta Ex5}$ was mainly localized in the cytoplasm, including axon and dendrite processes (Figure 1A). FLAG-MBNL1$^{\Delta Ex5}$ enhanced axon outgrowth by increasing primary and total axon length as well as the number of branch points as compared with control neurons (Figure 1B, 5 DIV). Similarly, the expression of FLAG-MBNL1$^{\Delta Ex5}$ in neurons at 11–14 DIV enhanced dendrite development by increasing total dendrite length and the number of primary dendrites (Figure 1B, 14 DIV). Expression of the nuclear isoform FLAG-MBNL1^{Ex5} did not promote axon outgrowth or neurite development; instead, the neurite outgrowth was impaired (Figures 1A and 1C).

We next wondered whether MBNL1 cytoplasmic localization was essential to dictate its function in promoting neurite differentiation. To test this, we generated an MBNL1^{Ex5} mutant construct with mutation at a predicted nuclear localization signal (NLS) from arginine to aspartic acid (FLAG-MBNL1^{Ex5}-R278D). The MBNL1^{Ex5} isoform mainly localized in the nucleus, whereas FLAG-MBNL1^{Ex5}-R278D distributed largely in the cytoplasm (Figures 1D and S1). Expression of the mutant FLAG-MBNL1^{Ex5}-R278D significantly improved the morphological defects: the total axon and dendrite length were comparable to that of control neurons (Figure 1D). Our results suggest that the MBNL1 cytoplasmic, but not nuclear, isoform promoted neurite differentiation and that the cytoplasmic localization may dictate its function.

Neurons with Reduced MBNL1 Level or Expressing Expanded CUG RNA Show Similar Defects in Axon Outgrowth and Dendrite Development

Early reduction of cytoplasmic MBNL1 on dendrites has been shown in the mouse brain expressing expanded CUG RNA (Wang et al., 2017), which is consistent with a notion that loss of MBNL1 cytoplasmic function is involved in DM1 neural pathogenesis. However, how MBNL1 cytoplasmic function is affected by expanded CUG RNA has not been investigated. We first determined the effect of expanded CUG RNA expression on axon and dendrite morphology. A vector expressing human *DMPK* 3′ UTR with 960 CUG RNA (DMPK-CUG^{960}) or without RNA repeats (DMPK-CUG^{0}) or control vector (pGW1) was co-transfected with a GFP-expression construct into hippocampal neurons. The primary and total axon length and number of branch points were lower in neurons expressing DMPK-CUG^{960} RNA than control vectors (Figure 2A). Similarly, in neurons expressing DMPK-CUG^{960} mRNA, the total dendrite length and primary dendrite number were reduced (Figure 2B), but the expression of control vector or DMPK-CUG^{0} mRNA did not affect dendrite development in cultured neurons. We further examined the total axon and dendrite length at different times after transfection and found that the impairment was likely due to DMPK-CUG^{960} RNA delaying axon outgrowth and dendrite development (Figures S2A–S2C). Thus, expanded CUG RNA may be toxic to neurons, and its expression delayed neurite maturation.

Figure 1. MBNL1 Cytoplasmic Isoform Promotes Neurite Morphogenesis

(A) The expression patterns of endogenous MBNL1, the transfected cytoplasmic isoform FLAG-MBNL1$^{\Delta Ex5}$, and nuclear isoform FLAG-MBNL1^{Ex5} in cultured hippocampal neurons at 5 and 14 DIV, as revealed by anti-MBNL1 and -FLAG immunoreactivity, respectively. At right: quantification of cytoplasm-to-nucleus ratio of MBNL1 or FLAG intensity. Arrows indicate nuclei of neurons expressing endogenous MBNL1. Arrowheads indicate nuclei of transfected neurons.

(B) FLAG-MBNL1$^{\Delta Ex5}$ expression in cultured hippocampal neurons enhances axon outgrowth (5 DIV) and dendrite development (14 DIV), with quantification at right.

(C) The expression of MBNL1 nuclear isoform (FLAG-MBNL1^{Ex5}) impaired axon outgrowth (5 DIV) and dendrite development (14 DIV), with quantification at right.

(D) Mutation in nuclear localization signal of FLAG-MBNL1^{Ex5} (FLAG-MBNL1^{Ex5}-R278D) increased cytoplasm-to-nucleus ratio of FLAG intensity and improved morphological defects in axon outgrowth (5 DIV) and dendrite development (14 DIV).

Number of neurons (n, from 3 individual cultured neuron preparations and transfections) used for quantification is indicated. Data are presented as mean ± SEM. $^{**}p < 0.01$; $^{***}p < 0.001$, by one way ANOVA in (A) and (D) and Student's t test in (B)–(D). Scale bars: 10 μm in (A) and 100 μm in (B)–(D). n.s., not significant.

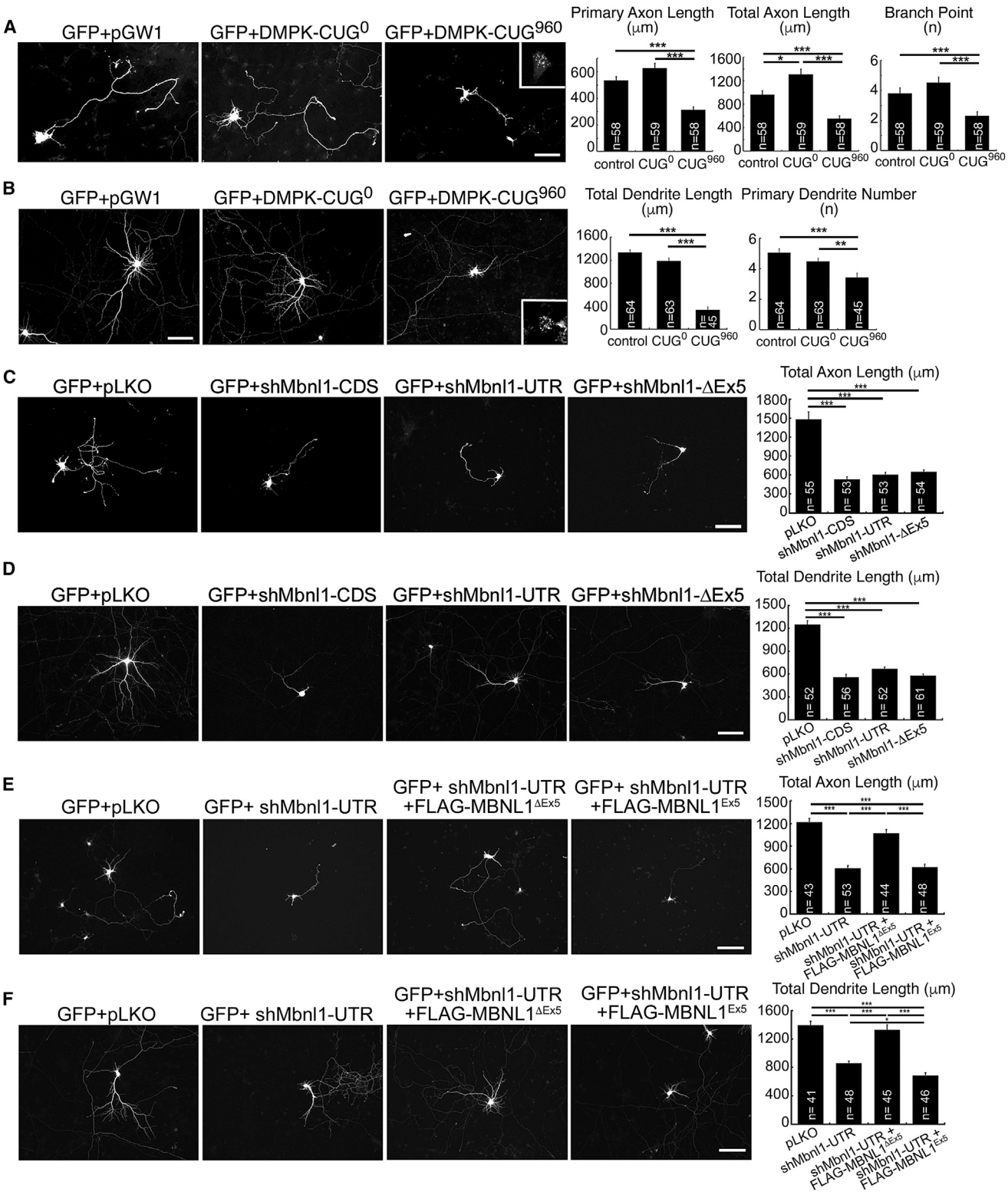

Figure 2. Expression of Expanded CUG mRNA or MBNL1 Knockdown in Neurons Causes Similar Defects in Axon Outgrowth and Dendrite Development

(A and B) Effect of expression of DMPK-CUG^{960} mRNA on axon outgrowth (A) and dendrite development (B) in cultured hippocampal neurons. Inset: RNA foci formation detected by *in situ* hybridization.

(legend continued on next page)

We next examined whether knockdown of MBNL1 caused similar defects in neurite outgrowth as in neurons expressing DMPK-CUG^{960} mRNA. We first used different *Mbnl1*-specific short hairpin RNA (shRNA) constructs targeted to the MBNL1 coding region or 3′ UTR to deplete both MBNL1 cytoplasmic and nuclear isoforms (Figure S2D). MBNL1 knocked-down neurons showed similarly impaired neurite outgrowth, including shorter total axon and dendrite length (Figures 2C and 2D, shMbnl1-CDS and shMbnl1-UTR). To determine whether cytoplasmic MBNL1 was important for neurite differentiation, we used another *Mbnl1* shRNA that preferentially depleted the MBNL1 cytoplasmic isoform (Figure S2E). Neurons with the depleted MBNL1 cytoplasmic isoform exhibited similar impairment in neurite outgrowth and reduced total axon and dendrite lengths (Figures 2C and 2D, shMbnl1-ΔEx5), which suggested that cytoplasmic MBNL1 was important for neurite morphogenesis. To further confirm this, we next determined whether re-expression of MBNL1 cytoplasmic isoform into Mbnl1-depleted neurons might rescue the morphological defects. Expression of the MBNL1 cytoplasmic, but not nuclear, isoform in Mbnl1-depleted neurons ameliorated the morphological impairment (Figures 2E and 2F). Therefore, defects in axon outgrowth and dendrite development were similar in neurons with MBNL1 knockdown and those expressing expanded CUG RNA, which suggests a pathogenic role for loss of MBNL function in the morphological phenotypes of DM1 neurons.

MBNL1 Cytoplasmic Isoform Rescues the Morphologic Defects in Neurons Expressing DMPK-CUG^{960} mRNA

We further determined whether loss of cytoplasmic MBNL1 contributed to the morphologic defects caused by CUG RNA repeats and whether overexpression of cytoplasmic MBNL1 could alleviate the morphological impairment. To test this, we overexpressed different amounts of MBNL1$^{\Delta Ex5}$ in neurons expressing DMPK-CUG^{960} mRNA: the ratio of plasmids expressing FLAG-MBNL1$^{\Delta Ex5}$ to DMPK-CUG^{960} was 1:1 or 2:1. The extent of improvement in neurite outgrowth was related to the amount of MBNL1$^{\Delta Ex5}$ overexpression (Figure 3). Excess expression of MBNL1$^{\Delta Ex5}$ rescued the neurite outgrowth defects: primary axon length, total axon length, and number of branch points were comparable to those of control neurons expressing DMPK-CUG^{0} mRNA (Figures 3A1–3A3 and 3B). A fraction of FLAG-MBNL1$^{\Delta Ex5}$ was still associated with nuclear RNA foci (Figures 3A5 and 3A6), which suggests that expanded CUG RNA also induced the sequestration of cytoplasmic MBNL1 into the nucleus.

We next wondered whether the rescue effect depended on the cytoplasmic localization of MBNL1. To test this, we co-expressed plasmids expressing DMPK-CUG^{960} mRNA and the MBNL1 nuclear isoform (FLAG-MBNL1^{Ex5}). Expression of FLAG-MBNL1^{Ex5} did not reverse the morphological defects caused by DMPK-CUG^{960} mRNA (Figures 3A4 and 3B). Thus, cytoplasmic, but not nuclear, MBNL1 reversed the morphological defects of neurons expressing DMPK-CUG^{960} mRNA, so loss of cytoplasmic MBNL1 may contribute to the histopathological abnormality caused by DMPK-CUG^{960} mRNA.

MBNL1 Localization to the Cytoplasm Is independent of Its Splicing Pattern

Alternative splicing of *Mbnl1* exon 5 is developmentally regulated in that increased exon 5 inclusion was observed during early developmental stages (Charizanis et al., 2012), which predicts a predominant nuclear localization for its encoded protein. On examining the endogenous distribution of MBNL1 in the developing brain at embryonic day (E)12.5, we found that it was mainly localized in the cytoplasm, whereas the percentage of exon 5 inclusion was greater in the E12.5 brain than in the adult brain (72% versus 42%) (Figures S3A and S3B). The results suggest that the alternative splicing pattern of MBNL1 was not consistent with its subcellular distribution. Similarly, in the EpA960/CaMKII-Cre mouse brain, reduced cytoplasmic MBNL1 occurred before aberrant alternative splicing (Wang et al., 2017), which suggests that the regulation is likely splicing independent.

Next, we determined the association of subcellular distribution and the *Mbnl1* exon 5 splicing pattern in cultured hippocampal neurons. Endogenous MBNL1 was mainly localized in the cytoplasm, whereas the *Mbnl1* exon 5 splicing pattern at 5 and 14 DIV revealed a similar developmental pattern of increased exon 5 inclusion (Figure S3C). Thus, although MBNL1 isoforms are generated from alternative splicing, an additional regulation is likely involved in controlling the subcellular localization.

Ubiquitination of MBNL1 Regulates Its Nucleocytoplasmic Localization

Because DMPK-CUG^{960} mRNA induced sequestration of FLAG-MBNL1$^{\Delta Ex5}$ from the cytoplasm into nuclear RNA foci (Figures 3A5 and 3A6), we next investigated the causal mechanism and determined whether this nuclear sequestration was due to cytoplasmic-to-nuclear translocation. Lysine 63-linked (K63) ubiquitination is known to regulate protein trafficking (Sims et al., 2012; Yang et al., 2009). To investigate whether MBNL1 cytoplasmic and nuclear localization are regulated by ubiquitination, we first determined whether MBNL1 was K63 ubiquitinated. FLAG-MBNL1$^{\Delta Ex5}$ was co-expressed with His-tagged ubiquitin wild-type (His-Ub-WT) or mutated lysine at 48 (K48R) or 63 (K63R) in HEK293T cells, and then underwent nickel-nitrilotriacetic acid (Ni-NTA) bead pull-down assay. MBNL1 was ubiquitinated (Figure 4A, lane 2). The extent of ubiquitination in cells expressing His-Ub-K63R was reduced, which suggests K63-linked ubiquitination (Figure 4A, lane 4). To confirm this, FLAG-MBNL1$^{\Delta Ex5}$ was co-transfected with hemagglutinin (HA)-tagged ubiquitin WT (HA-Ub-WT) or the K48 or K63 ubiquitin mutant with six

(C and D) MBNL1 knockdown impairs axon outgrowth (C) and dendrite development (D) in cultured hippocampal neurons. Three different shMbnl1 constructs targeting to coding region (shMbnl1-CDS), 3′ UTR (shMbnl1-UTR) and cytoplasmic isoform (shMbnl1-ΔEx5) were used in transfection.

(E and F) Expression of MBNL1 cytoplasmic, but not nuclear, isoform in Mbnl1-depleted cells with shMbnl1-UTR construct rescued the morphological defects in axon outgrowth (E) and dendrite development (F). Quantification of neurite morphologic features is also presented.

Number of neurons (n, from 3 individual cultured neuron preparations and transfections) used for quantification is indicated. Data are presented as mean ± SEM. *p < 0.05; **p < 0.01; ***p < 0.001, by one-way ANOVA. Scale bars: 100 μm.

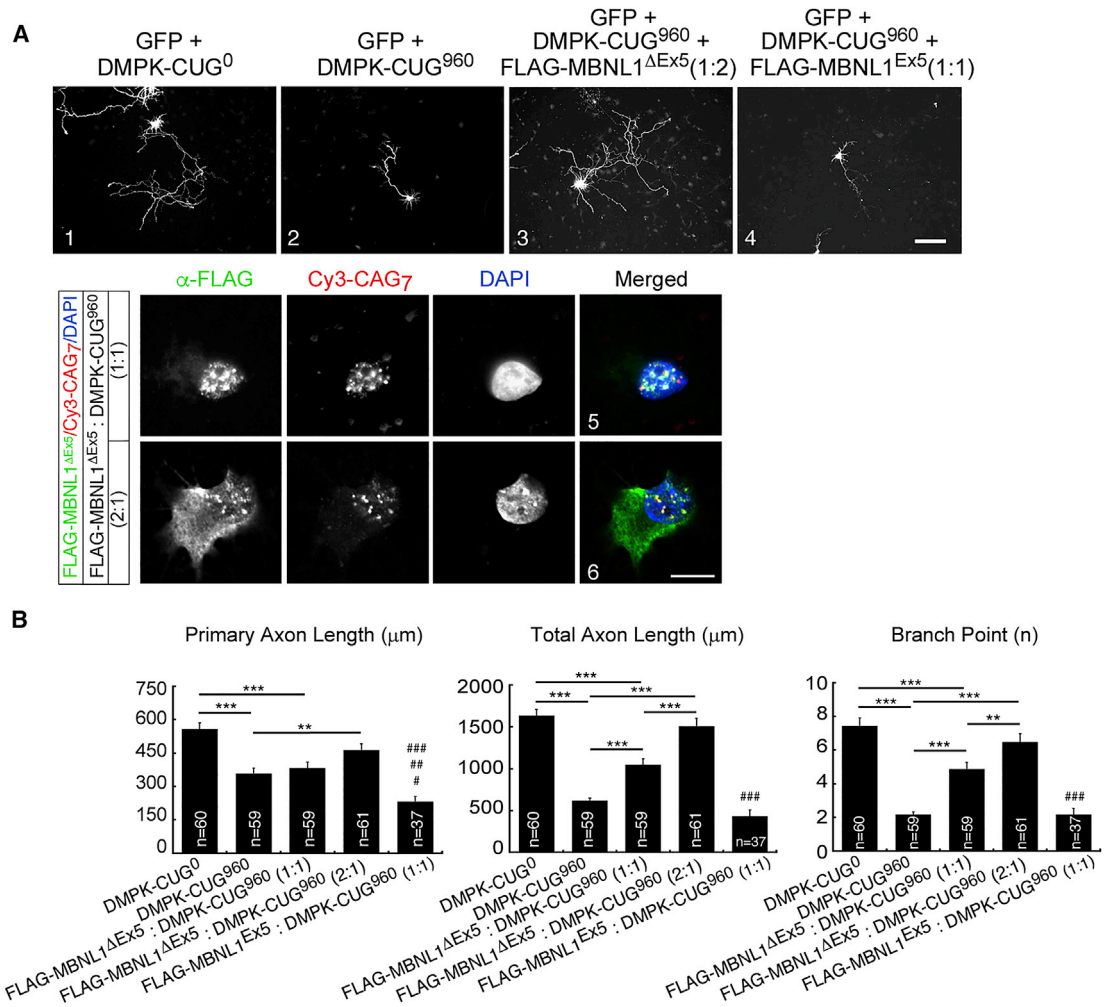

Figure 3. Overexpression of MBNL1 Cytoplasmic Isoform MBNL1$^{\Delta Ex5}$ Rescues the Morphologic Defects in Neurons Expressing DMPK-CUG^{960}

(A) Expression of MBNL1$^{\Delta Ex5}$, but not nuclear, isoform MBNL1^{Ex5} in neurons expressing DMPK-CUG^{960} mRNA rescued the morphological defects (1–4). Distribution of FLAG-tagged MBNL1$^{\Delta Ex5}$ with different transfected amounts of MBNL1$^{\Delta Ex5}$ (5 and 6).

(B) Quantification of neurite morphologic features from 3 independent experiments. Number of neurons used for quantification is indicated.

Data are presented as mean ± SEM. *p < 0.05; **p < 0.01; ***p < 0.001; $^{\#}$p < 0.05 versus transfection of plasmids expressing CUG^{960} mRNA, $^{\#\#}$p < 0.01 versus transfection of plasmids expressing FLAG-tagged MBNL1$^{\Delta Ex5}$ and DMPK-CUG^{960} (1:1); $^{\#\#\#}$p < 0.001 versus transfection of plasmids expressing DMPK-CUG^{0} or FLAG-tagged MBNL1$^{\Delta Ex5}$ and DMPK-CUG^{960} and (2:1) (primary axon length); $^{\#\#\#}$p < 0.001 versus all other transfection groups except DMPK-CUG^{960} group (total axon length and branch point), by one-way ANOVA. Scale bars: 100 μm in (A), 1–4, and 10 μm in (A), 5 and 6.

lysine residues substituted by arginines, except for lysine 48 or 63, in Neuro2A (N2A) cells. On immunoprecipitation (IP) with anti-FLAG antibody, MBNL1$^{\Delta Ex5}$ was ubiquitinated via K63 (Figure 4B).

We next investigated whether K63 ubiquitination regulated MBNL1 subcellular localization. First, we wondered whether K63 ubiquitination of MBNL1 dictating its cytoplasmic localization occurred for endogenous MBNL1 in the brain. To test this, we determined whether the extent of MBNL1 K63 ubiquitination differed in the cytoplasmic and nuclear fractions of the mouse brain. To enrich K63-ubiquitinated MBNL1, we used an ubiquitin affinity reagent, FLAG-tagged K63-selective tandem ubiquitin binding entity (Whitehurst et al., 1992) (FLAG-K63-TUBE) (Hjerpe et al., 2009), for IP (TUBE-IP). Mouse IgG and FLAG-K48-TUBE were included as controls for IP and the specificity of modification on lysine residue, respectively. In brain lysates from the cytoplasmic and nuclear fractions for TUBE-IP, K63-polyubiquitinated MBNL1 was present in the cytoplasmic fraction and was barely detected in the nuclear fraction, whereas mouse immunoglobulin G (IgG) or FLAG-K48-TUBE did not confer MBNL1 ubiquitination (Figures 4C, S4A, and S4B), which suggests that the cytoplasmic fraction of MBNL1 was largely K63 polyubiquitinated. The specificity of TUBE-IP signal recognized by anti-MBNL1 antibody was characterized and confirmed by IP and immunoblotting with the same antibody (Figure S4C). Moreover, consistent with the predominant cytoplasmic distribution in

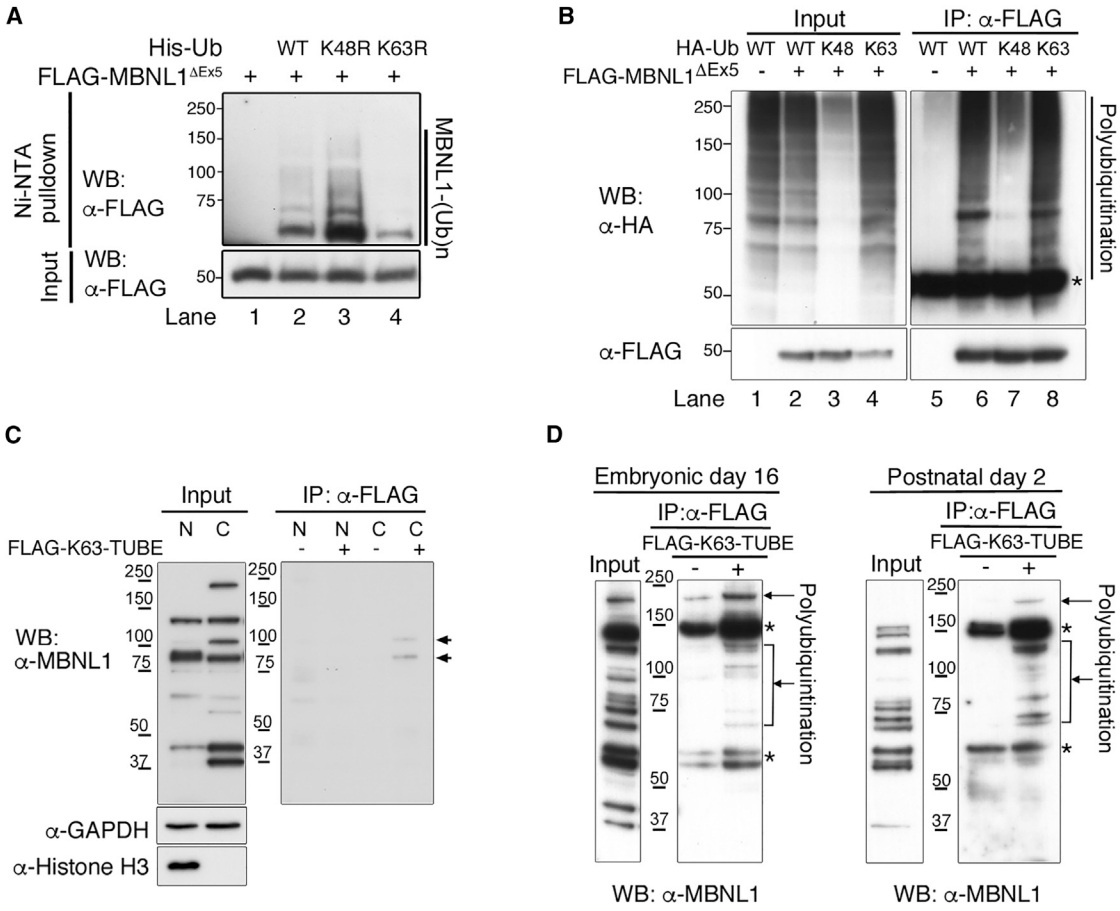

Figure 4. Ubiquitination of MBNL1 Regulates Its Nucleocytoplasmic Localization

(A) MBNL1 ubiquitination was through lysine (K)63. Immunoblot of lysed HEK293T cells transfected with FLAG-MBNL1$^{\Delta Ex5}$ along with His-ubiquitin (His-Ub), His-Ub K48R, or His-Ub K63R constructs, followed by Ni-NTA pull-down assay. WB, western blot.; WT, wild-type; Ni-NTA, nickel-nitrilotriacetic acid.

(B) MBNL1 was K63 polyubiquitinated. FLAG-MBNL1$^{\Delta Ex5}$ was co-transfected with different HA-tagged ubiquitin constructs in Neuro2A cells: WT, K48, and K63. Core MBNL1$^{\Delta Ex5}$ protein was revealed by anti-FLAG immunoreactivity. An asterisk represents the nonspecific signal from IgG after IP.

(C) K63-ubiquitinated MBNL1 was present in the cytoplasmic (C) fraction, but not the nuclear (N) fraction, of the mouse brain at 2 months of age. Lysates were incubated with FLAG-tagged K63-selective tandem ubiquitin binding entity (Flag-K63-TUBE) for immunoprecipitation (IP). Polyubiquitinated MBNL1 with molecular weight ~100 kDa is indicated by arrows. GAPDH and histone H3 were used as cytoplasmic and nuclear fraction markers, respectively.

(D) K63 ubiquitination of MBNL1 in developing mouse brains. Total lysates from brains at embryonic day 16 and post-natal day 2 were used for TUBE-IP. Arrows indicate polyubiquitinated MBNL1 with molecular weight >~60 kDa. Asterisks represent a non-specific signal that appeared in both groups.

developing mouse brain shown by immunofluorescence (Figure S3A), the extent of MBNL1 K63 ubiquitination in the developing mouse brain at E16.5 and post-natal day 2 seen on TUBE-IP also confirmed the K63-polyubiquitination of MBNL1 (Figure 4D).

We next generated MBNL1 constructs with mutations from lysine to arginine at predicted ubiquitination sites from bioinformatics analysis (FLAG-MBNL1$^{\Delta Ex5}$-K175R, -K246R, -K281R, and -K287R) and examined which residue may determine the cytoplasmic localization. As compared with the cytoplasmic distribution of MBNL1$^{\Delta Ex5}$, the ratio of cytoplasm-to-nucleus fraction of FLAG immunoreactivity was decreased in neurons expressing MBNL1$^{\Delta Ex5}$-K175R at 11–14 DIV or in N2A cells, whereas mutations at other residues did not change the cytoplasmic localization (Figures 5A and S5A). We next determined whether mutation at K175 also affected ubiquitination. Co-expression of FLAG-tagged MBNL1 constructs with His-tagged K63 ubiquitin (His-K63-Ub) in HEK293T cells, and followed by Ni-NTA bead pull-down assay, revealed that mutation at K175 reduced the extent of MBNL1 ubiquitination (Figure 5B). Similarly, co-expression of FLAG-tagged MBNL1 constructs with HA-Ub-WT in N2A cells followed by IP using anti-FLAG antibody also confirmed that mutation at K175 also reduced the extent of MBNL1 ubiquitination (Figure 5C). In addition, the nuclear translocation of MBNL1$^{\Delta Ex5}$-K175R impaired the function of MBNL1$^{\Delta Ex5}$ in promoting neurite outgrowth (Figure 5D). Thus, MBNL1 K63 ubiquitination may regulate its cytoplasmic localization.

We noticed that the K175 is located in the protein coding exon 3, which may indicate the availability of ubiquitination on the nuclear isoform MBNL1^{Ex5}. To test this possibility, we used the construct MBNL1^{Ex5}-Ub by tagging ubiquitin to the carboxyl

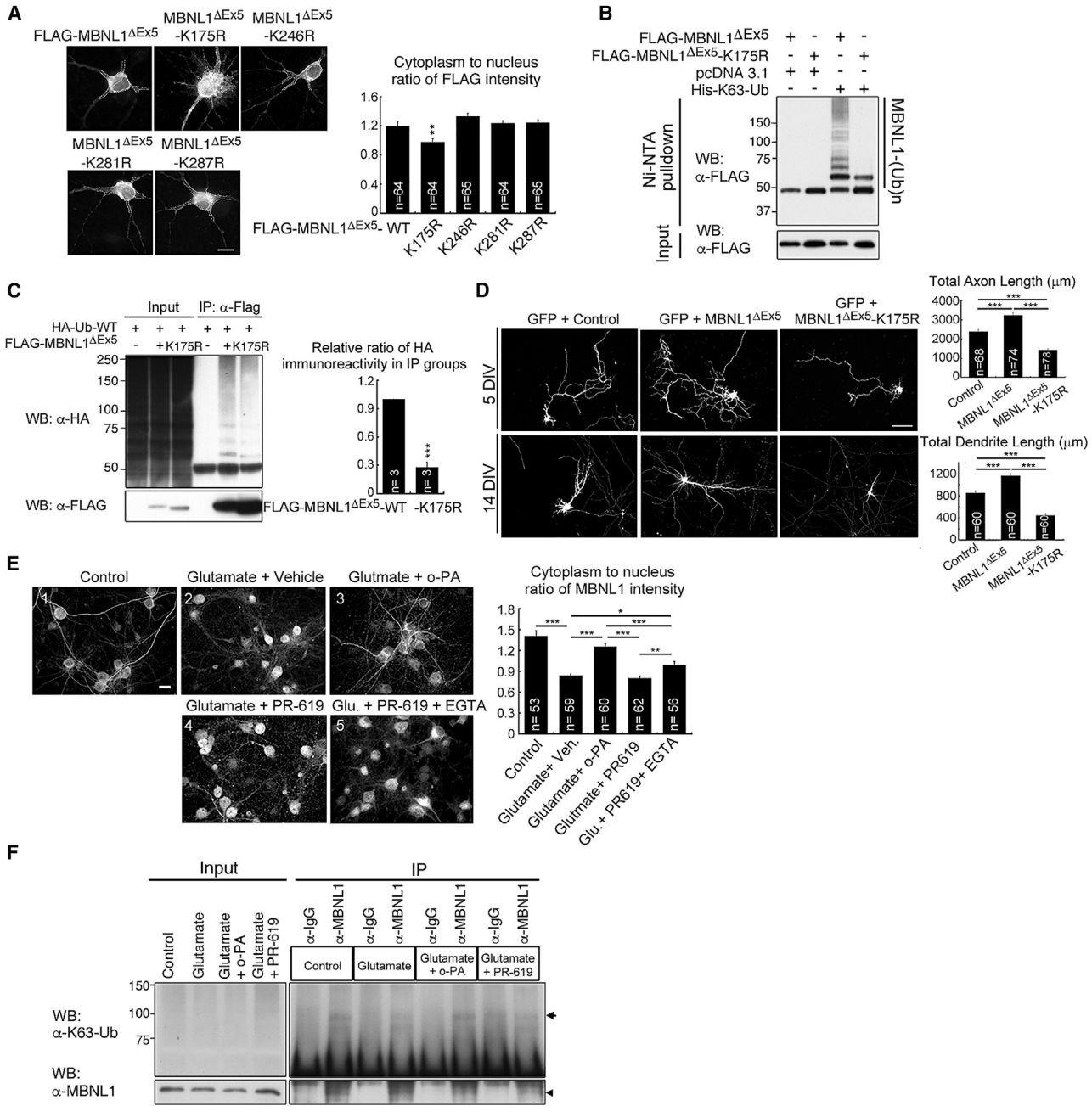

Figure 5. Ubiquitination of MBNL1 Is Required for Its Cytoplasmic Localization and Function

(A) Mutation at K175 decreased the cytoplasmic fraction of FLAG-MBNL1$^{\Delta Ex5}$. Quantification of cytoplasmic and nuclear distribution of MBNL1 mutants with different putative ubiquitination residues. Dotted lines outline the edge of the nucleus and cell body. WB, western blot.

(B and C) Mutation at K175 reduced the extent of MBNL1 ubiquitination. FLAG-MBNL1$^{\Delta Ex5}$ or FLAG-MBNL1$^{\Delta Ex5}$-K175R were co-transfected with His-K63-Ub in HEK293T cells followed by Ni-NTA pull-down assay (B). FLAG-MBNL1$^{\Delta Ex5}$ or FLAG-MBNL1$^{\Delta Ex5}$-K175R were co-transfected with HA-tagged ubiquitin constructs in Neuro2A cells followed by IP using anti-FLAG antibody (C). Quantification of the relative ratio of HA immunoreactivity in IP group is shown.

(D) Expression of FLAG-MBNL1$^{\Delta Ex5}$-K175R affected neurite morphology.

(E) Nuclear translocation of MBNL1 by glutamate treatment prevented by inhibiting the degradation of K63 polyubiquitin chain. o-PA, 1,10-phenanthroline. Quantification of cytoplasm-to-nucleus ratio of MBNL1 intensity is shown at right (n, number of neurons from 3 individual experiments).

(F) The o-PA pretreatment preserved the extent of K63-ubiquitinated MBNL1 in glutamate-treated neurons. Representative IP western blot analysis indicates the extent of K63-ubiquitinated MBNL1 with treatment. Cytoplasmic fractions from cultured neurons were used for IP. Arrow indicates polyubiquitinated MBNL1. Arrowhead indicates MBNL1$_{41/42}$.

Data are presented as mean ± SEM. $^{###}p < 0.001$ versus control; $^{*}p < 0.05$; $^{**}p < 0.01$; $^{***}p < 0.001$, one-way ANOVA in (A), (D), and (E) and Student's t test in (C). Scale bars: 10 μm in (A) and (E) and 100 μm in (D).

terminus of MBNL1^{Ex5} and determined whether promoting ubiquitination of MBNL1^{Ex5} affected its cytoplasmic distribution. MBNL1^{Ex5} ubiquitination increased the cytoplasmic distribution (Figure S5B) and reversed the impaired axon outgrowth as compared with MBNL1^{Ex5} (Figure S5C). Our results suggest that K63 ubiquitination may regulate the cytoplasmic localization of MBNL1.

To further confirm that modification by K63 ubiquitination was required for MBNL1 cytoplasmic localization, we knocked down endogenous Ubc13, an E2 ubiquitin-conjugating enzyme involved in the addition of the K63-linked polyubiquitin chain (Deng et al., 2000), because we did not have the candidate E3 ligase-controlled MBNL1 ubiquitination. Depletion of Ubc13 reduced the extent of MBNL1 ubiquitination in N2A cells (Figure S5D). As well, in cultured hippocampal neurons, depletion of Ubc13 resulted in decreased ratio of cytoplasm-to-nucleus fraction of MBNL1 immunoreactivity (Figure S5E), which supports the hypothesis that K63 ubiquitination of MBNL1 may dictate its cytoplasmic localization. Moreover, we determined the effect of K63 ubiquitination on FLAG-MBNL1$^{\Delta Ex5}$ protein stability by inhibiting protein synthesis with cycloheximide (CHX). At different times after CHX treatment, the level of FLAG-MBNL1$^{\Delta Ex5}$ protein (Figure S5F) and the extent of FLAG-MBNL1$^{\Delta Ex5}$ ubiquitination (Figure S5G) did not change, suggesting that K63 ubiquitination of MBNL1 may not cause MBNL1 degradation. Therefore, our results suggest that K63-linked ubiquitination regulated nucleocytoplasmic localization of MBNL1.

Ubiquitination-Mediated MBNL1 Nucleocytoplasmic Shuttling Was Activity Dependent

We next determined whether MBNL1 nucleocytoplasmic shuttling might be coordinated with neuronal activity. At 20 DIV, MBNL1 was distributed in both the cytoplasm and nucleus, and with glutamate treatment, it was localized in the nucleus (Figures 5E1 and 5E2). We next determined whether inhibition of endogenous deubiquitinase (DUB) activities would prevent the nuclear translocation. We used two inhibitors: (1) PR-619, a non-selective inhibitor of ubiquitin isopeptidases, which may increase overall protein polyubiquitination; or (2) 1,10-phenanthroline (o-PA), an inhibitor preventing degradation of K63-linked polyubiquitin chains by chelation of divalent metal ions. As indicated by the increased ratio of cytoplasm-to-nucleus fraction of MBNL1 immunoreactivity, the MBNL1 cytoplasmic fraction was increased in neurons treated with o-PA before glutamate treatment but not in those pre-treated with vehicle or PR-619 (Figures 5E2–5E4). The increase in cytoplasmic localization of MBNL1 in glutamate-treated neurons pretreated with o-PA was correlated with the increased extent of K63-ubiquitinated MBNL1 (Figure 5F). In contrast, the nuclear localization of MBNL1$^{\Delta Ex5}$-K175R impaired the function of MBNL1$^{\Delta Ex5}$ in promoting neurite outgrowth, which was not alleviated with o-PA treatment (Figure S5H). Thus, MBNL1 K63 ubiquitination may regulate its cytoplasmic localization and function.

The inhibition of MBNL1 nuclear translocation by PR-619, compared to that by o-PA, was ineffective (Figure 5E: control, 1.41 ± 0.07; vehicle pretreatment, 0.84 ± 0.02; PR-619 pretreatment, 0.80 ± 0.03), we wondered whether the inhibition may involve chelation of divalent metal ions. Pretreatment of combined PR-619 and EGTA partially prevented MBNL1 nuclear translocation on glutamate stimulation (Figure 5E5) (0.99 ± 0.05), which suggested that the activity of the unknown DUB may require divalent metal ions. In addition to inhibition of K63-specific DUBs, o-PA is also known to inhibit the DUB on proteasomes such as CSN5, also known as COP9 signalosome subunit 5 (Pulvino et al., 2015). To test whether the inhibitory effect of o-PA may be due to inhibition of CSN5 activity, we performed CSN5 knockdown in neurons and examined the subcellular localization of MBNL1 upon glutamate stimulation. CSN5 knockdown did not affect MBNL1 nuclear distribution in response to glutamate stimulation (Figures S6A and S6B), which suggests that CSN5 was not involved in regulating MBNL1 subcellular localization.

Moreover, the splicing pattern of *Mbnl1* exon 5 remained unchanged (Figure S6C) upon glutamate treatment, which suggests that this nuclear translocation was independent of splicing.

Misregulation of MBNL1 Ubiquitination Results in Nuclear Sequestration

A mouse model, EpA960/CaMKII-Cre, expressing expanded CUG RNA in the post-natal brain, recapitulates several features of the DM1 brain, including learning disability, neurodegeneration, and misregulation of alternative splicing (Wang et al., 2017). In the EpA960/CaMKII-Cre brain, reduced cytoplasmic MBNL1 expression on dendrites occurred before morphological degeneration and altered splicing. We wondered whether the reduced MBNL1 cytoplasmic content may be due to nuclear translocation and associated with a change in the level of K63-ubiquitinated MBNL1. To compare the extent of MBNL1 K63 ubiquitination, we used anti-MBNL1 antibody for IP and anti-ubiquitin K63-specific antibody for western blot analysis. Compared with control brains, EpA960/CaMKII-Cre brains showed a significantly reduced K63-ubiquitinated MBNL1 level in the cytosolic fraction (Figure 6A).

If the sequestration of cytoplasmic MBNL1 into nuclear RNA foci was due to deubiquitination resulting in a cytoplasmic-to-nuclear translocation, we wondered whether the nuclear translocation of MBNL1 could be reduced in neurons expressing DMPK-CUG^{960} RNA by (1) sustaining ubiquitination or (2) inhibiting deubiquitination of MBNL1. To sustain MBNL1 ubiquitination, we generated a constitutively ubiquitinated MBNL1 construct (MBNL1$^{\Delta Ex5}$-Ub) by tagging ubiquitin to the carboxyl terminus of MBNL1$^{\Delta Ex5}$. On co-transfection of equal amounts of plasmids expressing DMPK-CUG^{960} RNA and MBNL1$^{\Delta Ex5}$-Ub, although a fraction of MBNL1$^{\Delta Ex5}$-Ub was still associated with RNA foci, the cytoplasmic content was significantly increased (Figure 6B), as compared with the sequestration of MBNL1$^{\Delta Ex5}$ to nuclear RNA.

To inhibit MBNL1 deubiquitination, we treated neurons with o-PA to inhibit endogenous DUB activities at 12 hr after transfection to allow for expression of DMPK-CUG^{960} mRNA. Treatment with o-PA reduced the endogenous level of MBNL1 in the nucleus and increased that in the cytoplasm (Figure 6C). As well, the nuclear formation of RNA foci was reduced in neurons treated with o-PA (Figure 6C, inset), which supports the

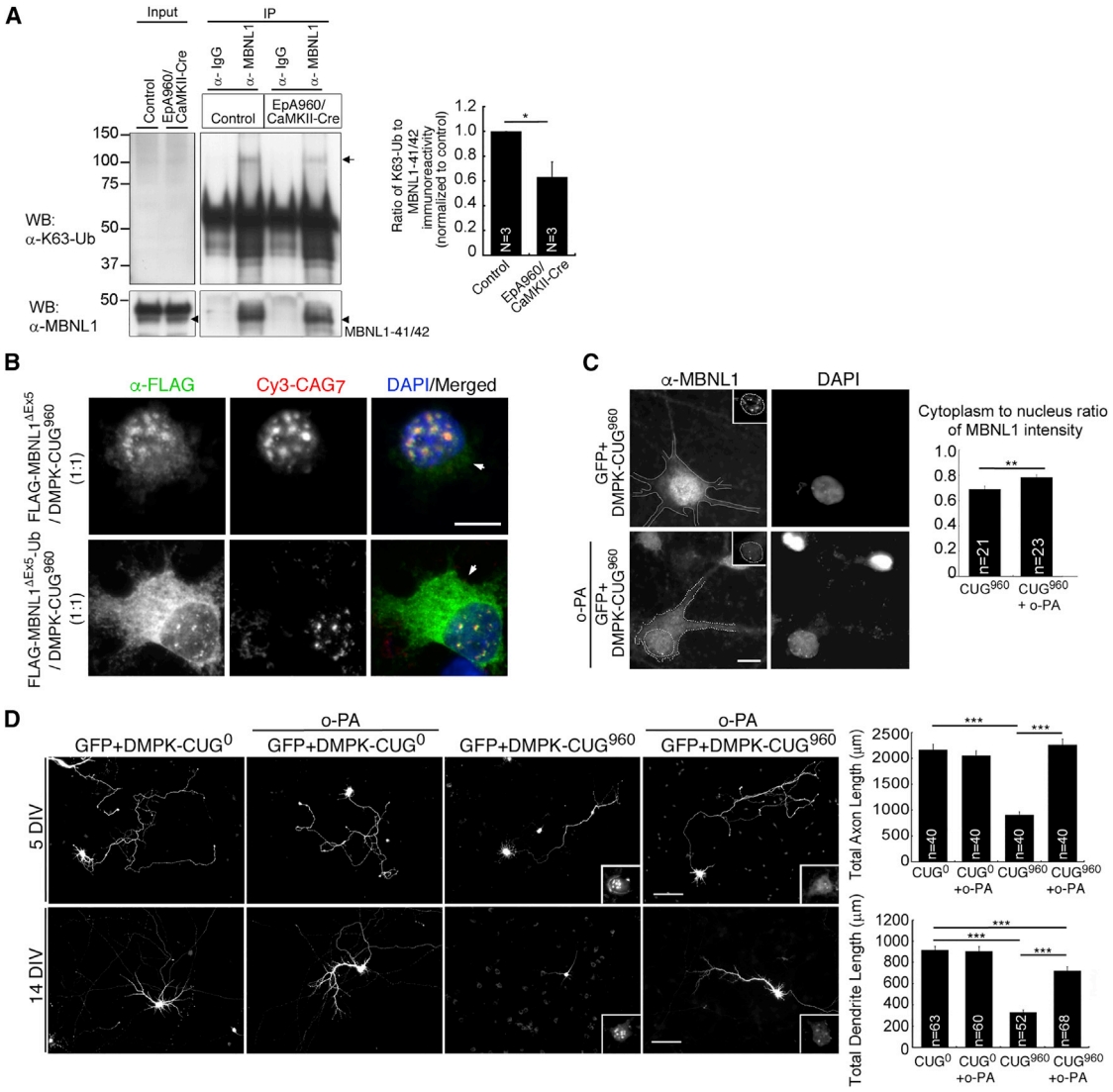

Figure 6. Ubiquitination of MBNL1 Preserved Its Cytoplasmic Localization and Neurite Morphology in Neurons Expressing DMPK-CUG^{960} mRNA

(A) Reduced K63-ubiquitinated MBNL1 in EpA960/CaMKII-Cre mouse brain. Representative IP western blot analysis indicates reduced K63-ubiquitinated MBNL1 in EpA960/CaMKII-Cre brains. Cytoplasmic fractions from 9-month-old brains were used for IP. Arrow indicates polyubiquitinated MBNL1. Arrowhead indicates MBNL1$_{41/42}$. Quantification of the relative ratio of K63-Ub immunoreactivity in IP group is shown at right.

(B) Expression of ubiquitin-tagged MBNL1 (FLAG-MBNL1$^{\Delta Ex5}$-Ub) increased the cytoplasmic fraction of MBNL1 in neurons expressing DMPK-CUG^{960} mRNA. Arrows indicate the cytoplasmic distribution of MBNL1.

(C) The o-PA treatment increased the cytoplasmic content of endogenous MBNL1 in neurons expressing DMPK-CUG^{960} mRNA. DAPI was used for nuclear staining. Dotted lines outline the edge of the nucleus and cell body. Inset: RNA foci detected by *in situ* hybridization. Quantification of cytoplasmic-to-nucleus ratio of MBNL1 intensity is shown.

(D) The o-PA treatment rescues the morphological impairment in neurons expressing DMPK-CUG^{960} mRNA. Inset: RNA foci detected by *in situ* hybridization. Quantification of neurite morphologic features is shown.

Number of neurons (n) used for quantification in (C) was from 2 individual cultured neuron preparations and transfections, and in (D), it was from 3 individual cultured neuron preparations and transfections. Data are presented as mean ± SEM. *p < 0.05; **p < 0.01; ***p < 0.001 by Student's t test in (A) and (C) and one-way ANOVA in (D). Scale bars: 10 μm in (B) and (C) and 100 μm in (D).

hypothesis that the association of MBNL1 with RNA foci is reversible. Treatment with o-PA for 48 hr significantly preserved the morphological features of neurons that expressed DMPK-CUG^{960} mRNA: total axon and dendrite length was increased as compared with no o-PA treatment, although the improvement in total dendrite length was not completely comparable to neurons expressing DMPK-CUG^{0} mRNA (Figure 6D). Our results suggest that expanded CUG RNA induced MBNL1 deubiquitination, which was impeded by inhibiting the activity of deubiquitinase.

In summary, cytoplasmic MBNL1 may play an important role in regulating neurite outgrowth, and its reduced expression in neurons expressing expanded CUG RNA is likely due to expanded CUG RNA-activated deubiquitination, resulting in nuclear translocation.

DISCUSSION

Emerging evidence supports an essential function for MBNL family proteins in regulating differentiation. Different MBNL isoforms are generated from alternative splicing, and the expression of spliced variants is developmentally regulated (Kanadia et al., 2006). Whether and how different MBNL isoforms, such as cytoplasmic and nuclear isoforms, contribute to differentiation has not been investigated. In addition, dysfunction of cytoplasmic MBNL1 has been implicated in DM1 pathogenesis (Miller et al., 2000; Wang et al., 2012), but how this leads to disease features is largely unclear. In this study, we showed that the cytoplasmic and nuclear isoforms of MBNL1 play distinct roles in regulating neurite differentiation; only the cytoplasmic—not the nuclear—isoform promoted neurite outgrowth. MBNL1 localization to the cytoplasm was regulated by K63-linked ubiquitination. MBNL1 mutation at a putative ubiquitination residue affected its cytoplasmic localization and impaired neurite outgrowth, so ubiquitination is required for the MBNL1 function in regulating neurite outgrowth. The expanded CUG RNA induced MBNL1 deubiquitination, thereby resulting in nuclear translocation and reduced MBNL1 cytoplasmic content and leading to morphological impairment. A mouse model, EpA960/CaMKII-Cre, expressing expanded CUG RNA in the brain showed reduced extent of MBNL1 ubiquitination, which is consistent with a previous finding of reduced MBNL1 cytoplasmic content on dendrites (Wang et al., 2017). Importantly, expanded CUG RNA induced MBNL1 nuclear translocation and morphological defects, which could be rescued by preventing degradation of K63-linked polyubiquitin chains or enhancing MBNL1 ubiquitination. Therefore, our findings provide the first evidence that the cytoplasmic function of MBNL1 is important for neurite morphogenesis and that deubiquitination of cytoplasmic MBNL1 is pathogenic in DM1 neurons. The pathogenic effect caused by deubiquitination of cytoplasmic MBNL1 may represent a novel mechanism for DM1 neural pathogenesis.

Our finding that post-translational modification by K63-linked ubiquitination or deubiquitination regulated the subcellular localization of MBNL1 is consistent with other reports that ubiquitination occurs primarily in the cytoplasmic compartment and is a regulatory mechanism for translocation between different compartments (Bonifacino and Weissman, 1998; Xu et al., 2010). Although the expression of the MBNL1 nuclear isoform did not enhance neurite outgrowth in cultured hippocampal neurons, the attempt to increase its cytoplasmic distribution by substituting the ubiquitin tag could still augment the function of promoting neurite outgrowth. Therefore, we postulated that both MBNL1 isoforms could be ubiquitinated and that localization of MBNL1 in the cytoplasm may be required for maintaining neuronal function and morphology.

In developing brains, MBNL1 polyubiquitination controls its cytoplasmic localization independent of the *Mbnl1* exon 5 splicing pattern. This finding is consistent with previous results that the *Mbnl1* exon 5 splicing pattern failed to reflect its subcellular localization during skeletal muscle development (Lin et al., 2006b), which also suggests an additional splicing-independent regulatory mechanism for controlling MBNL1 subcellular localization. Moreover, the detection of MBNL1 deubiquitination at 9 months, before the alternative splicing alteration in EpA960/CaMKII-Cre brains at 12 months (Wang et al., 2017), recapitulates the previous finding that early detection of PKC-mediated CELF1 hyperphosphorylation also occurs before the alternative splicing change in EpA960/MCM hearts (Wang et al., 2007). Accordingly, expanded CUG RNA may activate the signaling pathway in a tissue-specific manner to regulate post-translational modification of CELF1 or MBNL1, thereby resulting in the tissue-specific pathogenesis in DM1.

We showed that ubiquitination-mediated cytoplasmic localization of MBNL1 plays a role in promoting neurite outgrowth and maintaining neuronal morphologic features. Similar to loss of MBNL function, the expression of expanded CUG RNA also hindered neurite outgrowth or differentiation in cultured hippocampal neurons or PC12 cells (Quintero-Mora et al., 2002). How cytoplasmic MBNL1 promotes neurite outgrowth and the identification of molecules that regulate MBNL1 ubiquitination and deubiquitination are worthy of investigation. One of the possible regulatory mechanisms in controlling neurite morphogenesis and synaptic function would be via RNA localization and local translation (Mikl et al., 2010; Wang et al., 2012). For example, MBNL1 bound to the 3′ UTR of genes involved in regulating synaptic activity, such as CaMKIIα, Snap25, and integrin β1. In addition, MBNL1 distribution showed focal enrichment in the cell periphery or the structure with protrusion (Wang et al., 2012). Furthermore, a cytotoxic effect generated by glutamate treatment induced nuclear translocation of MBNL1, which suggests that (CUG)n RNA may elicit a stress-like response in neurons. How MBNL1 deubiquitination is activated, whether it is regulated by synaptic activity, and the signaling pathway that regulates this event need further investigation.

Approaches with antisense oligonucleotides and the development of small molecules have been effective in showing displacement of MBNL1 from nuclear CUG RNA foci and reversed splicing defects (Childs-Disney et al., 2013; Coonrod et al., 2013; Wheeler et al., 2012). Prevention of MBNL1 deubiquitination or maintaining MBNL1 ubiquitination may be an alternate approach to preserve the cytoplasmic function of MBNL1. Study to understand the regulation of nuclear and cytoplasmic shuttling of MBNL1 would provide important insights and another direction for developing a therapeutic strategy for the DM1 brain.

EXPERIMENTAL PROCEDURES

Ubiquitination Assay

The ubiquitination assays were performed as described elsewhere (Cheng et al., 2013). Briefly, HEK293T cells were transfected with the plasmids expressing FLAG-MBNL1$^{\Delta Ex5}$ or His-tagged wild-type or mutant ubiquitin for 24 hr and lysed using denatured buffer (buffer A: 6 M guanidine-HCl, 0.1 M Na_2HPO_4/NaH_2PO_4, 10 mM imidazole [pH 8.0]), followed by incubation with 20 μL Ni-NTA beads (QIAGEN) at room temperature for 1 hr. The beads were washed once with buffer A and buffer A mixed with buffer Ti (buffer Ti: 20 mM imidazole, 0.2% Triton X-100, 25 mM Tris-HCl [pH 6.8]) in a 1:3

dilution and three times with buffer Ti. Proteins were denatured by SDS sample buffer before SDS-PAGE and then underwent immunoblotting. To determine the effect of K63-linked ubiquitination on the stability of FLAG-MBNL1$^{\Delta Ex5}$, 24 hr after transfection, HEK293T cells were treated with 10 μM cycloheximide and harvested at different times for the Ni-NTA assay described earlier.

IP

For immunoprecipitation of HA-tagged ubiquitinated FLAG-MBNL1$^{\Delta Ex5}$ in N2A cells, 24 hr after transfection, cells were lysed with 1% Triton X-100 in PBS containing protease inhibitors, 1 mM EDTA, DNase I, RNase A, 10 mM DTT, 10 mM NEM, and 10 μM o-PA at 4°C for 1 hr. After centrifugation at 16,000 × *g*, the supernatant was pre-cleaned by incubation with magnetic Protein G beads for 10 min, followed by incubation with Protein G beads conjugated with anti-FLAG antibody 1 μg for 3 hr, washed with lysis buffer, and denatured by SDS sample buffer before SDS-PAGE.

IP of TUBE in Mouse Brains

Cerebral cortices and hippocampi from mouse brains were dounce homogenized by use of a loose pestle homogenizer with sucrose buffer (0.32 M sucrose, 10 mM 4-(2-hydroxyethyl)-1-piperazineethanesulfonic acid [HEPES], pH 7.5, 5 mM EDTA, with 10 μM o-PA, 10 mM DTT, 10 mM NEM, and protease inhibitors) (Huttner et al., 1983; Lin et al., 2006a). The crude nuclear and cytosolic fractions were separated by centrifugation at 800 × *g*. Before incubation for 1 hr with FLAG-K63-TUBE (LifeSensors), the P1 fraction underwent heavy grinding with a tight pestle, and DNase I and RNase A were added to both fractions for 30-min digestion at 4°C. The TUBE-incubated lysates underwent anti-FLAG antibody IP for 3 hr and washing 3 times with PBS.

For IP of endogenous MBNL1 in mouse brain, 200 μg protein lysates from a cytoplasmic fraction was used for IP. Briefly, lysates were pre-cleaned by incubation with magnetic Protein G beads for 10 min, followed by incubation with Protein G beads conjugated with anti-MBNL1 antibody 1 μg for overnight, washed with lysis buffer, and denatured by SDS sample buffer before SDS-PAGE.

Statistical Analysis

Data are presented as mean ± SEM and analyzed by using SigmaPlot 12.5 (Systat Software). Unpaired two-tailed Student's t test was used to compare 2 groups, and a one-way ANOVA was used to compare more than 2 groups, followed by Holm-Sidak multiple comparison tests. $p < 0.05$ was considered statistically significant. No statistical methods were used to pre-determine the sample size, but our sample sizes are similar to those reported in previous publications (Ramkhelawon et al., 2014; Sananbenesi et al., 2007). Data collection and analyses were not performed with blinding. The experiments were not randomized; cells on coverslips were randomly allocated to subjects for transfection only for each independent transfection in cultured neurons.

SUPPLEMENTAL INFORMATION

Supplemental Information includes Supplemental Experimental Procedures and six figures and can be found with this article online at https://doi.org/10.1016/j.celrep.2018.02.025.

ACKNOWLEDGMENTS

We thank Dr. Thomas Cooper (Baylor College of Medicine, Houston, TX, USA) for sharing reagents and Dr. Tang Tang for manuscript comments. This work was supported by grants from the Ministry of Science and Technology, Taiwan (NSC101-2321-B-001-017) and the Institute of Biomedical Sciences, Academia Sinica, Taiwan, to G.-S.W. and by a postdoctoral fellowship from Academia Sinica to T.-Y.K.

AUTHOR CONTRIBUTIONS

P.-Y.W., T.-Y.K., and G.-S.W. designed experiments. P.-Y.W., K.-T.C., Y.-M.L., T.-Y.K., and G.-S.W. performed experiments. P.-Y.W., K.-T.C., T.-Y.K., Y.-M.L., and G.-S.W. analyzed data. P.-Y.W., T.-Y.K., and G.-S.W. wrote the manuscript.

DECLARATION OF INTERESTS

The authors declare no competing interests.

Received: May 16, 2017
Revised: October 19, 2017
Accepted: February 6, 2018
Published: February 27, 2018

REFERENCES

Artero, R., Prokop, A., Paricio, N., Begemann, G., Pueyo, I., Mlodzik, M., Perez-Alonso, M., and Baylies, M.K. (1998). The muscleblind gene participates in the organization of Z-bands and epidermal attachments of Drosophila muscles and is regulated by Dmef2. Dev. Biol. *195*, 131–143.

Batra, R., Charizanis, K., Manchanda, M., Mohan, A., Li, M., Finn, D.J., Goodwin, M., Zhang, C., Sobczak, K., Thornton, C.A., and Swanson, M.S. (2014). Loss of MBNL leads to disruption of developmentally regulated alternative polyadenylation in RNA-mediated disease. Mol. Cell *56*, 311–322.

Bonifacino, J.S., and Weissman, A.M. (1998). Ubiquitin and the control of protein fate in the secretory and endocytic pathways. Annu. Rev. Cell Dev. Biol. *14*, 19–57.

Charizanis, K., Lee, K.Y., Batra, R., Goodwin, M., Zhang, C., Yuan, Y., Shiue, L., Cline, M., Scotti, M.M., Xia, G., et al. (2012). Muscleblind-like 2-mediated alternative splicing in the developing brain and dysregulation in myotonic dystrophy. Neuron *75*, 437–450.

Cheng, Y.C., Lin, T.Y., and Shieh, S.Y. (2013). Candidate tumor suppressor BTG3 maintains genomic stability by promoting Lys63-linked ubiquitination and activation of the checkpoint kinase CHK1. Proc. Natl. Acad. Sci. USA *110*, 5993–5998.

Cheng, A.W., Shi, J., Wong, P., Luo, K.L., Trepman, P., Wang, E.T., Choi, H., Burge, C.B., and Lodish, H.F. (2014). Muscleblind-like 1 (Mbnl1) regulates pre-mRNA alternative splicing during terminal erythropoiesis. Blood *124*, 598–610.

Childs-Disney, J.L., Stepniak-Konieczna, E., Tran, T., Yildirim, I., Park, H., Chen, C.Z., Hoskins, J., Southall, N., Marugan, J.J., Patnaik, S., et al. (2013). Induction and reversal of myotonic dystrophy type 1 pre-mRNA splicing defects by small molecules. Nat. Commun. *4*, 2044.

Coonrod, L.A., Nakamori, M., Wang, W., Carrell, S., Hilton, C.L., Bodner, M.J., Siboni, R.B., Docter, A.G., Haley, M.M., Thornton, C.A., and Berglund, J.A. (2013). Reducing levels of toxic RNA with small molecules. ACS Chem. Biol. *8*, 2528–2537.

Deng, L., Wang, C., Spencer, E., Yang, L., Braun, A., You, J., Slaughter, C., Pickart, C., and Chen, Z.J. (2000). Activation of the IkappaB kinase complex by TRAF6 requires a dimeric ubiquitin-conjugating enzyme complex and a unique polyubiquitin chain. Cell *103*, 351–361.

Du, H., Cline, M.S., Osborne, R.J., Tuttle, D.L., Clark, T.A., Donohue, J.P., Hall, M.P., Shiue, L., Swanson, M.S., Thornton, C.A., and Ares, M., Jr. (2010). Aberrant alternative splicing and extracellular matrix gene expression in mouse models of myotonic dystrophy. Nat. Struct. Mol. Biol. *17*, 187–193.

Goodwin, M., Mohan, A., Batra, R., Lee, K.Y., Charizanis, K., Fernández Gómez, F.J., Eddarkaoui, S., Sergeant, N., Buée, L., Kimura, T., et al. (2015). MBNL sequestration by toxic RNAs and RNA misprocessing in the myotonic dystrophy brain. Cell Rep. *12*, 1159–1168.

Han, H., Irimia, M., Ross, P.J., Sung, H.K., Alipanahi, B., David, L., Golipour, A., Gabut, M., Michael, I.P., Nachman, E.N., et al. (2013). MBNL proteins repress ES-cell-specific alternative splicing and reprogramming. Nature *498*, 241–245.

Hjerpe, R., Aillet, F., Lopitz-Otsoa, F., Lang, V., England, P., and Rodriguez, M.S. (2009). Efficient protection and isolation of ubiquitylated proteins using tandem ubiquitin-binding entities. EMBO Rep. *10*, 1250–1258.

Ho, T.H., Charlet-B, N., Poulos, M.G., Singh, G., Swanson, M.S., and Cooper, T.A. (2004). Muscleblind proteins regulate alternative splicing. EMBO J. *23*, 3103–3112.

Holm, F., Hellqvist, E., Mason, C.N., Ali, S.A., Delos-Santos, N., Barrett, C.L., Chun, H.J., Minden, M.D., Moore, R.A., Marra, M.A., et al. (2015). Reversion to an embryonic alternative splicing program enhances leukemia stem cell self-renewal. Proc. Natl. Acad. Sci. USA *112*, 15444–15449.

Huttner, W.B., Schiebler, W., Greengard, P., and De Camilli, P. (1983). Synapsin I (protein I), a nerve terminal-specific phosphoprotein. III. Its association with synaptic vesicles studied in a highly purified synaptic vesicle preparation. J. Cell Biol. *96*, 1374–1388.

Jiang, H., Mankodi, A., Swanson, M.S., Moxley, R.T., and Thornton, C.A. (2004). Myotonic dystrophy type 1 is associated with nuclear foci of mutant RNA, sequestration of muscleblind proteins and deregulated alternative splicing in neurons. Hum. Mol. Genet. *13*, 3079–3088.

Kanadia, R.N., Johnstone, K.A., Mankodi, A., Lungu, C., Thornton, C.A., Esson, D., Timmers, A.M., Hauswirth, W.W., and Swanson, M.S. (2003). A muscleblind knockout model for myotonic dystrophy. Science *302*, 1978–1980.

Kanadia, R.N., Shin, J., Yuan, Y., Beattie, S.G., Wheeler, T.M., Thornton, C.A., and Swanson, M.S. (2006). Reversal of RNA missplicing and myotonia after muscleblind overexpression in a mouse poly(CUG) model for myotonic dystrophy. Proc. Natl. Acad. Sci. USA *103*, 11748–11753.

Lin, C.W., Huang, T.N., Wang, G.S., Kuo, T.Y., Yen, T.Y., and Hsueh, Y.P. (2006a). Neural activity- and development-dependent expression and distribution of CASK interacting nucleosome assembly protein in mouse brain. J. Comp. Neurol. *494*, 606–619.

Lin, X., Miller, J.W., Mankodi, A., Kanadia, R.N., Yuan, Y., Moxley, R.T., Swanson, M.S., and Thornton, C.A. (2006b). Failure of MBNL1-dependent post-natal splicing transitions in myotonic dystrophy. Hum. Mol. Genet. *15*, 2087–2097.

Mikl, M., Vendra, G., Doyle, M., and Kiebler, M.A. (2010). RNA localization in neurite morphogenesis and synaptic regulation: current evidence and novel approaches. J. Comp. Physiol. A Neuroethol. Sens. Neural Behav. Physiol. *196*, 321–334.

Miller, J.W., Urbinati, C.R., Teng-Umnuay, P., Stenberg, M.G., Byrne, B.J., Thornton, C.A., and Swanson, M.S. (2000). Recruitment of human muscleblind proteins to (CUG)(n) expansions associated with myotonic dystrophy. EMBO J. *19*, 4439–4448.

Pascual, M., Vicente, M., Monferrer, L., and Artero, R. (2006). The Muscleblind family of proteins: an emerging class of regulators of developmentally programmed alternative splicing. Differentiation *74*, 65–80.

Pulvino, M., Chen, L., Oleksyn, D., Li, J., Compitello, G., Rossi, R., Spence, S., Balakrishnan, V., Jordan, C., Poligone, B., et al. (2015). Inhibition of COP9-signalosome (CSN) deneddylating activity and tumor growth of diffuse large B-cell lymphomas by doxycycline. Oncotarget *6*, 14796–14813.

Querido, E., Gallardo, F., Beaudoin, M., Ménard, C., and Chartrand, P. (2011). Stochastic and reversible aggregation of mRNA with expanded CUG-triplet repeats. J. Cell Sci. *124*, 1703–1714.

Quintero-Mora, M.L., Depardon, F., Waring, J., Korneluk, R.G., and Cisneros, B. (2002). Expanded CTG repeats inhibit neuronal differentiation of the PC12 cell line. Biochem. Biophys. Res. Commun. *295*, 289–294.

Ramkhelawon, B., Hennessy, E.J., Ménager, M., Ray, T.D., Sheedy, F.J., Hutchison, S., Wanschel, A., Oldebeken, S., Geoffrion, M., Spiro, W., et al. (2014). Netrin-1 promotes adipose tissue macrophage retention and insulin resistance in obesity. Nat. Med. *20*, 377–384.

Rau, F., Freyermuth, F., Fugier, C., Villemin, J.P., Fischer, M.C., Jost, B., Dembele, D., Gourdon, G., Nicole, A., Duboc, D., et al. (2011). Misregulation of miR-1 processing is associated with heart defects in myotonic dystrophy. Nat. Struct. Mol. Biol. *18*, 840–845.

Sananbenesi, F., Fischer, A., Wang, X., Schrick, C., Neve, R., Radulovic, J., and Tsai, L.H. (2007). A hippocampal Cdk5 pathway regulates extinction of contextual fear. Nat. Neurosci. *10*, 1012–1019.

Sims, J.J., Scavone, F., Cooper, E.M., Kane, L.A., Youle, R.J., Boeke, J.D., and Cohen, R.E. (2012). Polyubiquitin-sensor proteins reveal localization and linkage-type dependence of cellular ubiquitin signaling. Nat. Methods *9*, 303–309.

Suenaga, K., Lee, K.Y., Nakamori, M., Tatsumi, Y., Takahashi, M.P., Fujimura, H., Jinnai, K., Yoshikawa, H., Du, H., Ares, M., Jr., et al. (2012). Muscleblind-like 1 knockout mice reveal novel splicing defects in the myotonic dystrophy brain. PLoS ONE *7*, e33218.

Sznajder, L.J., Michalak, M., Taylor, K., Cywoniuk, P., Kabza, M., Wojtkowiak-Szlachcic, A., Matłoka, M., Konieczny, P., and Sobczak, K. (2016). Mechanistic determinants of MBNL activity. Nucleic Acids Res. *44*, 10326–10342.

Tran, H., Gourrier, N., Lemercier-Neuillet, C., Dhaenens, C.M., Vautrin, A., Fernandez-Gomez, F.J., Arandel, L., Carpentier, C., Obriot, H., Eddarkaoui, S., et al. (2011). Analysis of exonic regions involved in nuclear localization, splicing activity, and dimerization of Muscleblind-like-1 isoforms. J. Biol. Chem. *286*, 16435–16446.

Wang, G.S., Kearney, D.L., De Biasi, M., Taffet, G., and Cooper, T.A. (2007). Elevation of RNA-binding protein CUGBP1 is an early event in an inducible heart-specific mouse model of myotonic dystrophy. J. Clin. Invest. *117*, 2802–2811.

Wang, E.T., Cody, N.A., Jog, S., Biancolella, M., Wang, T.T., Treacy, D.J., Luo, S., Schroth, G.P., Housman, D.E., Reddy, S., et al. (2012). Transcriptome-wide regulation of pre-mRNA splicing and mRNA localization by muscleblind proteins. Cell *150*, 710–724.

Wang, P.Y., Lin, Y.M., Wang, L.H., Kuo, T.Y., Cheng, S.J., and Wang, G.S. (2017). Reduced cytoplasmic MBNL1 is an early event in a brain-specific mouse model of myotonic dystrophy. Hum. Mol. Genet. *26*, 2247–2257.

Wheeler, T.M., Leger, A.J., Pandey, S.K., MacLeod, A.R., Nakamori, M., Cheng, S.H., Wentworth, B.M., Bennett, C.F., and Thornton, C.A. (2012). Targeting nuclear RNA for in vivo correction of myotonic dystrophy. Nature *488*, 111–115.

Whitehurst, C., Henney, H.R., Max, E.E., Schroeder, H.W., Jr., Stüber, F., Siminovitch, K.A., and Garrard, W.T. (1992). Nucleotide sequence of the intron of the germline human kappa immunoglobulin gene connecting the J and C regions reveals a matrix association region (MAR) next to the enhancer. Nucleic Acids Res. *20*, 4929–4930.

Xu, G., Paige, J.S., and Jaffrey, S.R. (2010). Global analysis of lysine ubiquitination by ubiquitin remnant immunoaffinity profiling. Nat. Biotechnol. *28*, 868–873.

Yang, W.L., Wang, J., Chan, C.H., Lee, S.W., Campos, A.D., Lamothe, B., Hur, L., Grabiner, B.C., Lin, X., Darnay, B.G., and Lin, H.K. (2009). The E3 ligase TRAF6 regulates Akt ubiquitination and activation. Science *325*, 1134–1138.

Yuan, Y., Compton, S.A., Sobczak, K., Stenberg, M.G., Thornton, C.A., Griffith, J.D., and Swanson, M.S. (2007). Muscleblind-like 1 interacts with RNA hairpins in splicing target and pathogenic RNAs. Nucleic Acids Res. *35*, 5474–5486.